Acta Crystallographica Section F
**Structural Biology and Crystallization Communications**
ISSN 1744-3091

# Crystallization and preliminary X-ray analysis of the receiver domain of a putative response regulator, BPSL0128, from *Burkholderia pseudomallei*

**Abd Ghani Abd Aziz,[a] Svetlana E. Sedelnikova,[a] Sergey N. Ruzheinikov,[a] Simon Thorpe,[b] Rahmah Mohamed,[c,d] Sheila Nathan,[c,d] John B. Rafferty,[a] Patrick J. Baker[a] and David W. Rice[a]***

[a]Krebs Institute for Biomolecular Research, Department of Molecular Biology and Biotechnology, The University of Sheffield, Sheffield S10 2TN, England, [b]Department of Chemistry, The University of Sheffield, Sheffield S3 7HF, England, [c]School of Biosciences and Biotechnology, Faculty of Science and Technology, Universiti Kebangsaan Malaysia, 43600 Bangi, Selangor D.E., Malaysia, and [d]Malaysia Genome Institute, Jalan Bangi, 43000 Kajang, Selangor D.E., Malaysia

Correspondence e-mail: d.rice@sheffield.ac.uk

Received 30 March 2012
Accepted 6 June 2012

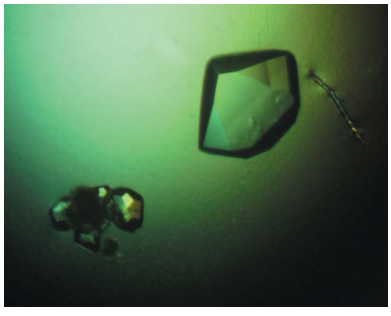



*bpsl0128*, a gene encoding a putative response regulator from *Burkholderia pseudomallei* strain D286, has been cloned into a pETBLUE-1 vector system, overexpressed in *Escherichia coli* and purified. The full-length protein is degraded during purification to leave a fragment corresponding to the putative receiver domain, and crystals of this protein that diffracted to beyond 1.75 Å resolution have been grown by the hanging-drop vapour-diffusion technique using PEG 6000 as the precipitant. The crystals belonged to one of the enantiomorphic pair of space groups $P3_121$ and $P3_221$, with unit-cell parameters $a = b = 65.69$, $c = 105.01$ Å and either one or two molecules in the asymmetric unit.

## 1. Introduction

*Burkholderia pseudomallei*, previously known as *Pseudomonas pseudomallei* (Leelarasamee, 1986), is a motile, aerobic, non-spore-forming, Gram-negative bacillus (White, 2003) found in hot wet soils in Southeast Asia and northern Australia (Wuthiekanun *et al.*, 2005; Currie *et al.*, 2008). This bacterium has the ability to adapt and survive across a range of adverse environmental conditions (Stevens & Galyov, 2004) and is the causative agent of melioidosis, a disease which is endemic in these regions. However, the distribution of the pathogen may be more geographically widespread, as the disease is not statutorily notifiable in many countries (Dance, 2000). It has been suggested that the higher incidence of disease observed during the monsoon and rainy seasons is possibly a consequence of the rise in the water table bringing bacteria from underlying soils to the surface (Chaowagul *et al.*, 1989; Brett & Woods, 2000). Common routes of infection by *Burkholderia* are either by the contact of wounds with contaminated soil or water or by the ingestion or inhalation of contaminated airborne soil particles (Songsivilai & Dharakul, 2000). Following infection, the manifestation of the disease varies greatly from an asymptomatic state to an overwhelming septicaemia (Woods *et al.*, 1999). Particular risk factors for individuals susceptible to developing the disease include diabetes mellitus, chronic renal disease, chronic lung disease, alcoholism and HIV infection (Cheng & Currie, 2005). Early identification of the disease is of paramount importance so that an effective chemotherapeutic strategy can be implemented in a timely fashion to achieve a good outcome and to eradicate the disease (Brett & Woods, 2000).

For an organism to thrive and cause infection, it has to have the ability to overcome the immune defences of the host, to grow under nutrient-limiting conditions and to respond to hostile factors in the environment (Barrett & Hoch, 1998). In order to invade, survive and adapt in such conditions, bacteria frequently use two-component signal transduction systems (TCSTs) to control the expression of target genes that determine the nature of the cellular response to the particular challenge (Hecht *et al.*, 1995; Barrett & Hoch, 1998; Barrett *et al.*, 1998). TCSTs are very widespread in prokaryotes, but are less abundant in eukaryotes (Alex & Simon, 1994; Loomis *et al.*, 1997, 1998; Chang & Stewart, 1998; Stock *et al.*, 2000; Schaller *et al.*, 2011).

TCSTs have been reported to play an important role in antibiotic resistance towards vancomycin in staphylococci and enterococci (Cosgrove *et al.*, 2004; Hong *et al.*, 2008), towards tetracycline in *Bacteroides* strains (Rasmussen & Kovacs, 1993) and towards penicillin in *Streptococcus pneumoniae* (Guenzi *et al.*, 1994). TCSTs are composed of a sensor histidine kinase (HK) protein (40–110 kDa) and a response regulator (RR) protein (∼25 kDa; Milani *et al.*, 2005). In response to a signal, a histidine residue on the sensor kinase is autophosphorylated, promoting its interaction with its cognate RR by transfer of the phosphoryl group to a conserved aspartate residue on the RR receiver domain and thus activating a specific response (Stock *et al.*, 1989). The widespread distribution of TCSTs has led to the suggestion that they might form attractive targets for the development of novel antibacterial agents by targeting either the HK or the RR proteins and therefore interfering with intracellular signalling networks to the detriment of the bacteria (Goldschmidt *et al.*, 1997; Stock *et al.*, 2000).

The HKs can be divided into three major groups: (i) periplasmic sensing HKs with sensory and kinase domains that are located in two different cellular compartments separated by a membrane and connected by at least two transmembrane helices, (ii) HKs that have sensing mechanisms associated with membrane-spanning helices and (iii) cytoplasmic sensing HKs that are either soluble or membrane-anchored (Mascher *et al.*, 2006). Most HKs, such as EnvZ from *Escherichia coli*, are membrane-anchored (Jung *et al.*, 2001), but exceptions include the chemotaxis kinase CheA and the nitrogen-regulatory kinase NtrB, both of which are soluble cytoplasmic proteins (Alex & Simon, 1994; Stock *et al.*, 2000; Mascher *et al.*, 2006). Sequence comparisons show that the HK components of the TCST superfamily from different species of bacteria share a number of common sequence motifs, including the residues that make up the H, N, D, F and G boxes that form important components of the active site (Wolanin *et al.*, 2002).

The majority of RRs consist of two domains. The first of these, usually corresponding to the N-terminal ∼120 residues, forms a receiver domain which shows a high degree of sequence and structural homology across the superfamily. In contrast, the C-terminal region, which encodes the DNA-binding domain, is highly variable (Feher *et al.*, 1997; West & Stock, 2001). In some RRs, for example CheY and Spo0F, the C-terminal DNA-binding domain is absent (Stock *et al.*, 1989). The receiver domain adopts a $(\beta\alpha)_5$ fold composed of a five-stranded $\beta$-sheet with two $\alpha$-helices on one face of the $\beta$-sheet and three on the other (Lubetsky & Stock, 2005). The characteristic feature of this domain is an acidic pocket that contains the phospho-accepting aspartate residue (Allen *et al.*, 2001). The nature of the DNA-binding domain has been used to conveniently classify the various RRs into subfamilies corresponding to (i) a winged-helix domain (*e.g.* OmpR), (ii) a four-helix domain (*e.g.* NarL) and (iii) an ATPase-coupled helix–turn–helix domain (*e.g.* NtrC) (Stock *et al.*, 1989, 2000).

Sequence analysis has shown that *B. pseudomallei* contains the genes for at least 52 two-component signal transduction systems (Holden *et al.*, 2004). One of these genes, *bpsl0127*, corresponds to a putative histidine kinase and is adjacent to that for a response regulator, *bpsl0128* (Chong *et al.*, 2006). The C-terminal domain of BPSL0128 shows strong sequence similarity to the DNA-binding domain of *Aquifex aeolicus* NtrC4, which contains a classical helix–turn–helix motif. However, whilst NtrC4 possesses an ATPase domain between the receiver and DNA-binding domains, this is missing in BPSL0128 (Batchelor *et al.*, 2008). In this paper, we report the production, crystallization and preliminary X-ray analysis of crystals of the putative receiver domain of BPSL0128.

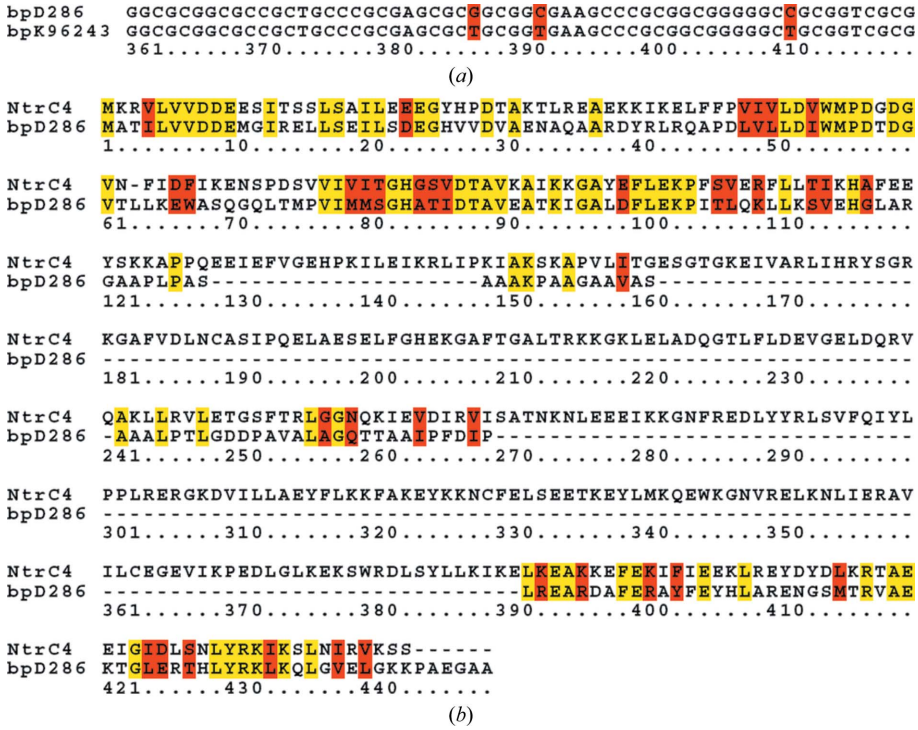


**Figure 1**
(*a*) Sequence alignment of the *bpsl0128* region of *B. pseudomallei* strains D286 (bpD286) and K96243 (bpK96243), in which three nucleotide differences can be seen (highlighted in red). The alignment was generated using *Biology Workbench* 3.2 (http://workbench.sdsc.edu). The bottom line represents the numbers of the bases in the coding sequence (left justified). (*b*) Sequence alignment of BPSL0128 from *B. pseudomallei* strain D286 (bpD286) and NtrC4 from *A. aeolicus*. Identical residues are coloured yellow; similar residues are coloured red.

## 2. Materials and methods

### 2.1. Cloning and overexpression

Genomic DNA was purified from a pathogenic strain of *B. pseudomallei* strain D286 isolated from a melioidosis patient at Kuala Lumpur General Hospital (Lee *et al.*, 2007). The gene encoding the 227-residue protein BPSL0128 was PCR-amplified from the primers 5′-ATG GCA ACC ATC CTG GTG-3′ (forward) and 5′-AAA AAA TTT ATG CCG CGC CTT-3′ (reverse) designed on the basis of the *B. pseudomallei* K96243 sequence (Holden *et al.*, 2004). PCR was carried out using a DyNazyme EXT PCR kit (Finnzymes); owing to the highly GC-rich nature of the *B. pseudomallei* DNA, an additional 5% DMSO was added to the PCR mixture (Chakrabarti & Schutt, 2001). The PCR amplification was carried out over 25 cycles in order to reduce the probability of mutation. DNA fragments were purified using a QIAquick Gel Extraction Kit (Qiagen) and ligated into the pETBLUE-1 vector using an AccepTor vector kit (Novagen). Positive transformants were identified by blue/white screening and colony PCR.

Plasmid DNA was isolated, sequenced and compared with the gene sequence of *bpsl0128* from *B. pseudomallei* strain K96243, revealing three nucleotide differences (Fig. 1*a*). To rule out the possibility that these differences arose from chance mutations during PCR, the cloning was repeated and the consistency of the sequence variation was confirmed by DNA sequencing. Compared with *bpsl0128* from strain K96243, two of the mutations in strain D286 are silent, while the third results in the replacement of Val131 by alanine. Analysis (*BLAST*) of the *bpsl0128* sequence from strain D286 shows that it is identical to the homologue from *B. pseudomallei* strain 1106a. Sequence alignment of BPSL0128 against NtrC4 shows that the receiver and DNA-binding domains of each are closely related (Fig. 1*b*).

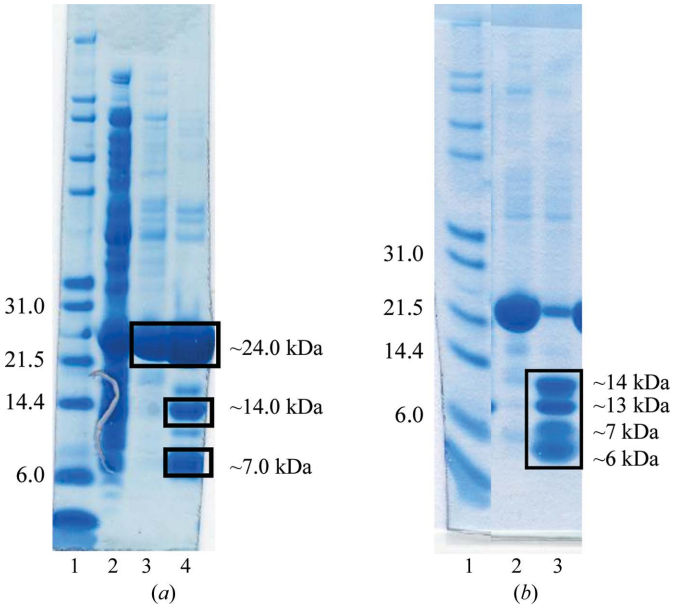


**Figure 2**
(*a*) SDS–PAGE (NuPAGE 4–12% BT gel, Invitrogen) showing stages in the purification of recombinant *B. pseudomallei* BPSL0128. Lane 1, Mark12 (Invitrogen; labelled in kDa); lane 2, cell-free extract; lane 3, pooled fractions from HiTrap Heparin HP column; lane 4, pooled fractions from RESOURCE Q column. (*b*) SDS–PAGE (NuPAGE 4–12% BT gel, Invitrogen) showing the degradation of BPSL0128 after purification. Lane 1, Mark12 (Invitrogen; labelled in kDa); lane 2, pooled fractions after the HiTrap Heparin HP column; lane 3, BPSL0128 after storage for 4 d at room temperature. The highlighted box in lane 3 shows four bands arising from protein degradation.

The plasmid was transformed into *E. coli* Tuner (DE3) pLacI (Novagen). The protein was overexpressed by inoculating a 250 ml flask containing 50 ml Luria–Bertani (LB) broth supplemented with 50 µg ml$^{-1}$ carbenicillin and 34 µg ml$^{-1}$ chloramphenicol with a single colony. The culture was grown overnight at 310 K on a shaking tray (250 rev min$^{-1}$). In order to produce sufficient protein for structural studies, 5 ml of the starter culture was used to inoculate 500 ml LB broth medium in a 2 l flask supplemented as above. The flasks were incubated at 310 K until an $OD_{600}$ of 0.6 was reached, when overexpression was induced by the addition of 1 m*M* IPTG followed by incubation for a further 4 h. The cells were harvested by centrifugation at 18 600*g* at 277 K (JLA-10.500 rotor, Avanti J-25I, Beckman) and stored at 253 K.

### 2.2. Purification

The cell pellets were defrosted, resuspended in about eight volumes of 50 m*M* Tris pH 8.0 and disrupted by sonication using a Soniprep 150 machine set at 16 µm amplitude over two cycles of 20 s each. Cell debris was removed by centrifugation at 70 000*g* for 10 min (JA-25.50 rotor, Avanti J25I Beckman). The supernatant fraction was loaded onto a 5 ml HiTrap Heparin HP column (GE Healthcare) and proteins were eluted using a 40 ml linear gradient of NaCl from 0.1 to 0.6 *M* in 50 m*M* Tris pH 8.0. BPSL0128 eluted at about 0.25 *M* NaCl and fractions containing significant quantities were pooled, diluted threefold with water and loaded onto a 6 ml RESOURCE Q (GE Healthcare) column. BPSL0128 eluted from this column at approximately 0.2 *M* NaCl when a 60 ml linear gradient of NaCl from 0.1 to 0.3 *M* in 50 m*M* Tris pH 8.0 was applied. An attempt to purify the protein further using gel filtration on a HiLoad 16/60 Superdex 200 column in 50 m*M* Tris pH 8.0, 0.5 *M* NaCl did not improve the purity significantly and subsequent protocols therefore omitted this step. The elution position of BPSL0128 on gel filtration suggested that the apparent molecular weight of the protein in solution was about 90 kDa, suggesting that BPSL0128 is a tetramer. SDS–PAGE analysis showed a strong band around 24 kDa corresponding to BPSL0128, but a degree of degradation was indicated as two major bands at 14 and 7 kDa could be observed (Fig. 2*a*). Further studies in which the protein was left at room temperature for 4 d showed that the 24 kDa band was rapidly degraded into multiple smaller protein fragments (approximately 14, 13, 7 and 6 kDa; Fig. 2*b*). N-terminal sequence analysis of these bands was performed on a Procise 491 Protein Sequencing System (Applied Biosystems) after blotting on a

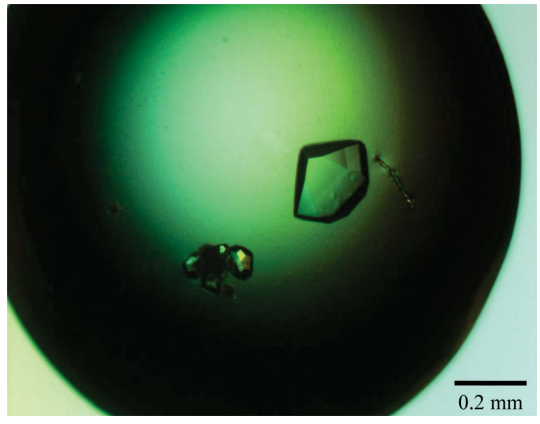


**Figure 3**
Crystals of the putative response regulator receiver domain of *B. pseudomallei* BPSL0128 grown from 16%(*w*/*v*) PEG 6000, 0.1 *M* Tris pH 7.5, 0.2 *M* calcium chloride.

polyvinylidene fluoride (PVDF) membrane. This showed that the 14 and 13 kDa bands represented fragments with Ala2 at the N-terminus (ATILV). The third (7 kDa) band corresponded to a mixture of two small fragments, 60% of which started with Ala157 (AGQTTAAI) and 40% with Ala144 (ALPTLGDD). The N-terminal sequence of the 6 kDa band showed that this fragment started with Thr161 (TAAIPFDI).

### 2.3. Crystallization of the regulator protein

Prior to crystallization, pooled samples of purified full-length protein were concentrated using a Vivaspin centrifugal concentrator with a 10 kDa molecular-weight cutoff filter (Sartorius, Germany) and the buffer was exchanged to 10 m*M* Tris pH 8.0 using a diafiltration cup. The final protein concentration was approximately 19 mg ml$^{-1}$ (Bradford, 1976). Preliminary crystallization conditions were screened with NeXtal suites (JCSG+ and PACT suites from Qiagen) using the vapour-diffusion sitting-drop strategy on a Matrix Hydra II Plus One crystallization robot (Thermo Fisher Scientific, USA) by adding 0.2 µl protein solution at 13 mg ml$^{-1}$ in 10 m*M* Tris–HCl pH 8.0 to the same volume of precipitant and equilibrating against a 40 µl reservoir of the same precipitant at 289 K. Small crystals were observed after 7 d using 0.1 *M* Tris pH 7.5, 0.2 *M* calcium chloride, 20%(*w*/*v*) PEG 6000 as the precipitant. Optimization of these conditions by manual screening using the hanging-drop vapour-diffusion technique led to the growth of larger trigonal crystals (0.2 × 0.2 × 0.2 mm; Fig. 3) in 0.1 *M* Tris pH 7.5, 0.2 *M* calcium chloride, 16%(*w*/*v*) PEG 6000 using a 2:1 ratio of protein to precipitant. N-terminal sequencing was carried out on the crystals and confirmed that the sequence started with Ala2 (ATILV). Further crystals were harvested along with some mother liquor and dissolved in 10% acetic acid for further analysis by liquid-chromatography mass spectrometry (LC-MS). The sample was loaded onto an Acquity UPLC (Waters) liquid chromatograph fitted with a BEH C18 column (1.7 µm, 2.1 × 500 mm; Waters) and eluted with a gradient of 5–95% acetonitrile in 0.1% formic acid at 400 µl min$^{-1}$ over 7 min. Two major peaks were observed in the elution profile (Fig. 4*a*). The eluent was directly coupled to an LCT Premier XE (Waters) mass spectrometer fitted with an orthogonal electrospray ionization (ESI) source to determine the mass of each peak. The multiply charged ion array from one peak was deconvoluted (*MaxEnt* software) and indicated that the predominant protein mass was 13 743 Da (Fig. 4*b*). This mass, together with the identification of the N-terminal sequence of the crystallized fragment, indicates that it corresponds to residues 2–128, with the observed and expected molecular weights differing by only 0.2 Da. These residues form the putative receiver domain of BPSL0128 and this indicates that cleavage has occurred at the boundary of this domain and the linker which connects it to the DNA-binding domain. The second broad peak was shown to consist of a series of peaks with molecular weights ranging from ∼5700 to ∼6300 Da (Fig. 4*c*). In line with the results from the protein sequencing, we believe that this peak corresponds to fragments of the DNA-binding domain.

### 2.4. Harvesting crystals and data collection

Crystals were transferred to a cryoprotectant solution containing 35% glycerol together with the relevant concentration of the precipitant and flash-cooled to 100 K in a liquid-nitrogen cold stream. Crystals were tested for diffraction using an in-house X-ray Rigaku MicroMax-007 copper rotating-anode generator fitted with Varimax

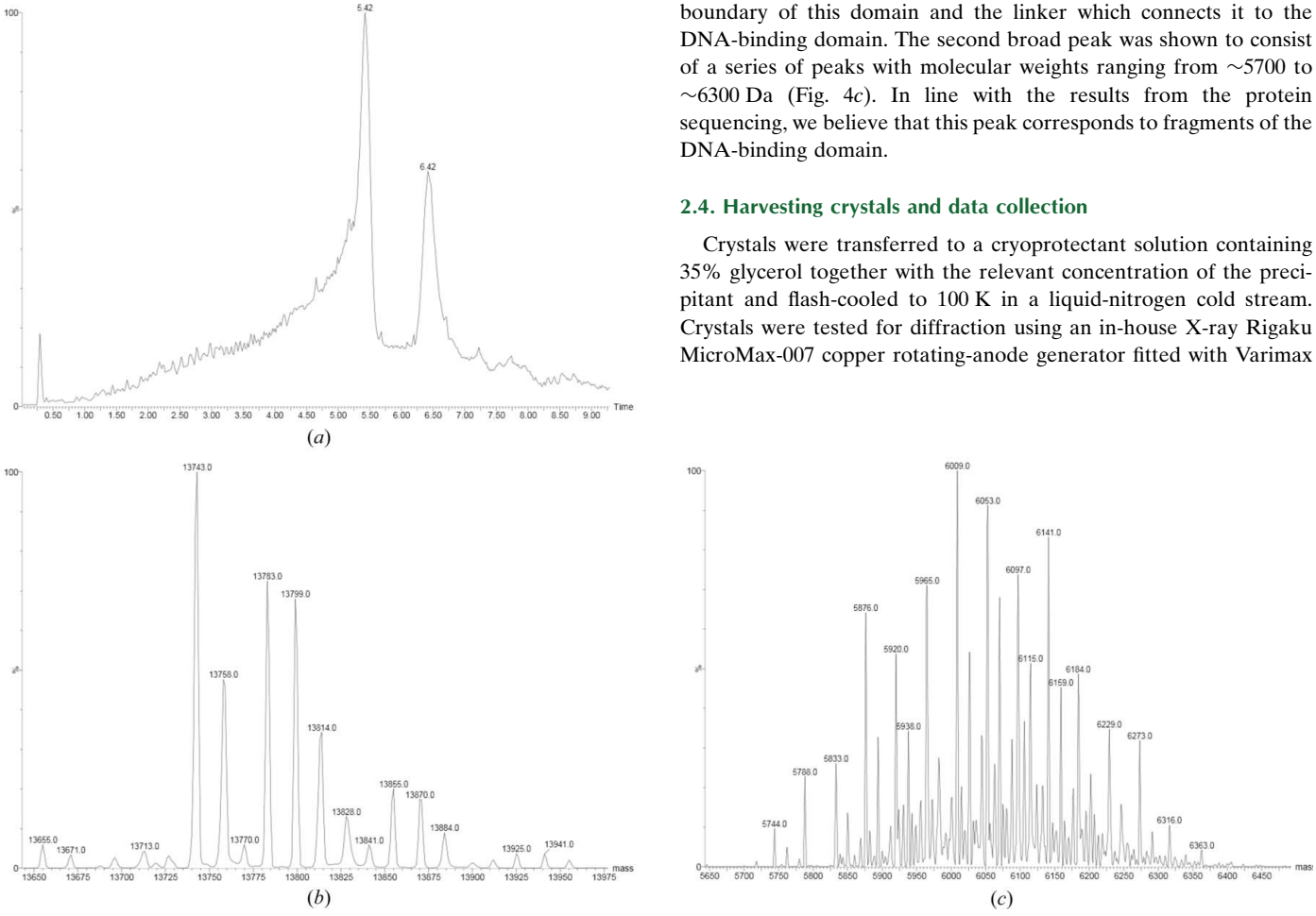


**Figure 4**
(*a*) Liquid-chromatographic analysis of harvested crystals and their surrounding mother liquor following crystallization of the putative response regulator receiver domain of *B. pseudomallei* BPSL0128. The *x* axis of the chromatogram corresponds to time in minutes and the *y* axis indicates the signal intensity. The peak eluting at 6.42 min represents the crystallized fragment and corresponds to the putative receiver domain. The peak eluting at 5.42 min is believed to correspond to residues from the DNA-binding domain. (*b*) Chromatogram of the mass-spectrometric analysis of the sample eluting at 6.42 min, indicating a mass of 13 743 Da (*x* axis). (*c*) Chromatogram of the mass-spectrometric analysis of the sample eluting at 5.42 min, indicating heterogeneous populations of fragments with masses around 6000 Da.

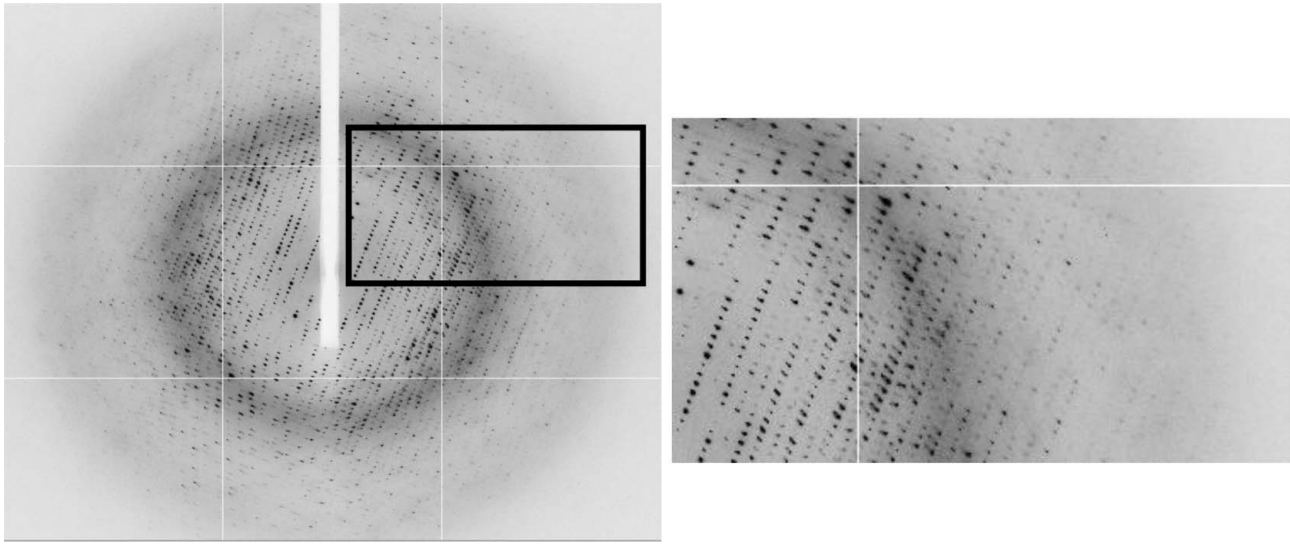

**Figure 5**
A representative 1° oscillation image of data collected from a native crystal of the putative response regulator receiver domain of BPSL0128 using an ADSC Q315 detector on beamline I03 at Diamond Light Source, Oxford, England. An enlarged view of the region indicated by the square is shown on the right. The diffraction extended to 1.75 Å resolution. Data-processing statistics can be found in Table 1.

**Table 1**
X-ray data-collection statistics for native crystals of the *B. pseudomallei* putative response regulator receiver domain.

Values in parentheses are for the highest resolution shell.

| | |
|---|---|
| Wavelength (Å) | 0.9763 |
| Space group | $P3_121$ or $P3_221$ |
| Unit-cell parameters (Å) | $a = b = 65.69$, $c = 105.01$ |
| Temperature (K) | 100 |
| X-ray source | I03, Diamond Light Source |
| Detector | ADSC Q315 |
| Resolution (Å) | 29.81–2.00 (2.11–2.00) |
| Unique reflections | 18164 (2622) |
| $R_{\rm merge}$† | 0.052 (0.182) |
| Completeness (%) | 99.4 (99.8) |
| Multiplicity | 10.3 (10.2) |
| Mean $I/\sigma(I)$ | 27.7 (11.3) |

† $R_{\rm merge} = \sum_{hkl}\sum_i |I_i(hkl) - \langle I(hkl)\rangle| / \sum_{hkl}\sum_i I_i(hkl)$, where $I_i(hkl)$ and $\langle I(hkl)\rangle$ are the observed intensity and the mean intensity of related reflections, respectively.

confocal optics and a MAR Research image plate. Crystals that diffracted well were stored and data were collected to 1.75 Å resolution using an ADSC Q315 CCD detector and an 80 µm beam on beamline I03 at the Diamond Light Source (180 images of 1° oscillation; Fig. 5).

## 3. Results and discussion

Preliminary analysis of the diffraction data using the autoindexing routine in *iMOSFLM* (Leslie, 1992; Leslie & Powell, 2007; Battye *et al.*, 2011) showed that the crystals of the putative receiver domain belonged to a primitive trigonal space group, with unit-cell parameters $a = b = 65.69$, $c = 105.01$ Å. Despite indications from the diffraction pattern (Fig. 5) that the spots were split, a high-quality native data set was obtained to a resolution of 2.0 Å following processing using *xia2* (Winter, 2010) utilizing the *XDS*/*XSCALE* (Kabsch, 2010) and *SCALA* (Winn *et al.*, 2011) packages. Analysis of the pattern of systematic absences was consistent with the crystal belonging to one of the enantiomorphic pair of space groups $P3_121$ and $P3_221$. Data-collection and processing statistics are shown in Table 1. Calculation of possible values of $V_{\rm M}$, assuming that the crystallized protein has a molecular weight of 13.7 kDa as determined by mass spectrometry, indicated that the asymmetric unit contains one or two subunits, with $V_{\rm M}$ values of 4.8 or 2.4 Å$^3$ Da$^{-1}$, respectively (Matthews, 1968, 1976). Attempts are now being made to solve the structure of the putative receiver domain of BPSL0128 using sulfur-SAD in the hope of obtaining a better understanding of response regulators in general and this protein in particular.

RM, SN and DWR acknowledge the Ministry of Science, Technology and Innovation, Government of Malaysia (grant 07-05-16-MGI-GMB08) and the British Council PMI-2 Initiative for financial support. We acknowledge the Diamond Synchrotron for provision of beamtime and thank James Nicholson for assistance with station I03. AGAA thanks Universiti Putra Malaysia and the Ministry of Higher Education Malaysia for scholarship funding.

## References

Alex, L. A. & Simon, M. I. (1994). *Trends Genet.* **10**, 133–138.
Allen, M. P., Zumbrennen, K. B. & McCleary, W. R. (2001). *J. Bacteriol.* **183**, 2204–2211.
Barrett, J. F. *et al.* (1998). *Proc. Natl Acad. Sci. USA*, **95**, 5317–5322.
Barrett, J. F. & Hoch, J. A. (1998). *Antimicrob. Agents Chemother.* **42**, 1529–1536.
Batchelor, J. D., Doucleff, M., Lee, C. J., Matsubara, K., De Carlo, S., Heideker, J., Lamers, M. H., Pelton, J. G. & Wemmer, D. E. (2008). *J. Mol. Biol.* **384**, 1058–1075.
Battye, T. G. G., Kontogiannis, L., Johnson, O., Powell, H. R. & Leslie, A. G. W. (2011). *Acta Cryst.* D**67**, 271–281.
Bradford, M. M. (1976). *Anal. Biochem.* **72**, 248–254.
Brett, P. J. & Woods, D. E. (2000). *Acta Trop.* **74**, 201–210.
Chakrabarti, R. & Schutt, C. E. (2001). *Gene*, **274**, 293–298.
Chang, C. & Stewart, R. C. (1998). *Plant Physiol.* **117**, 723–731.
Chaowagul, W., White, N. J., Dance, D. A., Wattanagoon, Y., Naigowit, P., Davis, T. M., Looareesuwan, S. & Pitakwatchara, N. (1989). *J. Infect. Dis.* **159**, 890–899.
Cheng, A. C. & Currie, B. J. (2005). *Clin. Microbiol. Rev.* **18**, 383–416.
Chong, C.-E., Lim, B.-S., Nathan, S. & Mohamed, R. (2006). *In Silico Biol.* **6**, 341–346.
Cosgrove, S. E., Carroll, K. C. & Perl, T. M. (2004). *Clin. Infect. Dis.* **39**, 539–545.

Currie, B. J., Dance, D. A. B. & Cheng, A. C. (2008). *Trans. R. Soc. Trop. Med. Hyg.* **102**, S1–S4.
Dance, D. A. (2000). *Acta Trop.* **74**, 115–119.
Feher, V. A., Zapf, J. W., Hoch, J. A., Whiteley, J. M., McIntosh, L. P., Rance, M., Skelton, N. J., Dahlquist, F. W. & Cavanagh, J. (1997). *Biochemistry*, **36**, 10015–10025.
Goldschmidt, R. M., Macielag, M. J., Hlasta, D. J. & Barrett, J. F. (1997). *Curr. Pharm. Des.* **3**, 125–142.
Guenzi, E., Gasc, A. M., Sicard, M. A. & Hakenbeck, R. (1994). *Mol. Microbiol.* **12**, 505–515.
Hecht, G. B., Lane, T., Ohta, N., Sommer, J. M. & Newton, A. (1995). *EMBO J.* **14**, 3915–3924.
Holden, M. T. *et al.* (2004). *Proc. Natl Acad. Sci. USA*, **101**, 14240–14245.
Hong, H.-J., Hutchings, M. I. & Buttner, M. J. (2008). *Adv. Exp. Med. Biol.* **631**, 200–213.
Jung, K., Hamann, K. & Revermann, A. (2001). *J. Biol. Chem.* **276**, 40896–40902.
Kabsch, W. (2010). *Acta Cryst.* D**66**, 125–132.
Lee, S.-H., Chong, C.-E., Lim, B.-S., Chai, S.-J., Sam, K.-K., Mohamed, R. & Nathan, S. (2007). *Diagn. Microbiol. Infect. Dis.* **58**, 263–270.
Leelarasamee, A. (1986). *J. Infect. Dis. Antimicrob. Agents*, **3**, 84–93.
Leslie, A. G. W. (1992). *Jnt CCP4/ESF–EAMCB Newsl. Protein Crystallogr.* **26**.
Leslie, A. G. W. & Powell, H. R. (2007). *Evolving Methods for Macromolecular Crystallography*, edited by R. J. Read & J. L. Sussman, pp. 41–51. Dordrecht: Springer.
Loomis, W. F., Kuspa, A. & Shaulsky, G. (1998). *Curr. Opin. Microbiol.* **1**, 643–648.
Loomis, W. F., Shaulsky, G. & Wang, N. (1997). *J. Cell Sci.* **110**, 1141–1145.
Lubetsky, J. B. & Stock, A. M. (2005). *Structural Biology of Bacterial Pathogenesis*, edited by G. Waksman, M. Caparon & S. Hultgren, pp. 17–22. Washington: ASM Press.
Mascher, T., Helmann, J. D. & Unden, G. (2006). *Microbiol. Mol. Biol. Rev.* **70**, 910–938.
Matthews, B. W. (1968). *J. Mol. Biol.* **33**, 491–497.
Matthews, B. W. (1976). *Annu. Rev. Phys. Chem.* **27**, 493–523.
Milani, M., Leoni, L., Rampioni, G., Zennaro, E., Ascenzi, P. & Bolognesi, M. (2005). *Structure*, **13**, 1289–1297.
Rasmussen, B. A. & Kovacs, E. (1993). *Mol. Microbiol.* **7**, 765–776.
Schaller, G. E., Shiu, S.-H. & Armitage, J. P. (2011). *Curr. Biol.* **21**, R320–R330.
Songsivilai, S. & Dharakul, T. (2000). *Acta Trop.* **74**, 169–179.
Stevens, M. P. & Galyov, E. E. (2004). *Int. J. Med. Microbiol.* **293**, 549–555.
Stock, A. M., Robinson, V. L. & Goudreau, P. N. (2000). *Annu. Rev. Biochem.* **69**, 183–215.
Stock, J. B., Ninfa, A. J. & Stock, A. M. (1989). *Microbiol. Rev.* **53**, 450–490.
West, A. H. & Stock, A. M. (2001). *Trends Biochem. Sci.* **26**, 369–376.
White, N. J. (2003). *Lancet*, **361**, 1715–1722.
Winn, M. D. *et al.* (2011). *Acta Cryst.* D**67**, 235–242.
Winter, G. (2010). *J. Appl. Cryst.* **43**, 186–190.
Wolanin, P. M., Thomason, P. A. & Stock, J. B. (2002). *Genome Biol.* **3**, reviews301.
Woods, D. E., DeShazer, D., Moore, R. A., Brett, P. J., Burtnick, M. N., Reckseidler, S. L. & Senkiw, M. D. (1999). *Microbes Infect.* **1**, 157–162.
Wuthiekanun, V., Mayxay, M., Chierakul, W., Phetsouvanh, R., Cheng, A. C., White, N. J., Day, N. P. J. & Peacock, S. J. (2005). *J. Clin. Microbiol.* **43**, 923–924.